

Supporting Information (SI) for Salts of 1-(Chloromethyl)-1,1-dimethylhydrazine and Ionic Liquids

by Carles Miró Sabaté,* Henri Delalu, Valérian Forquet and Erwann Jeanneau

Experimental Section

General Method

All solvents and chemicals were used as supplied by Sigma-Aldrich Inc. and/or Fisher Scientific without further purification. Sodium 5,5'-azotetrazolate pentahydrate,¹ barium 5,5'-azotetrazolate pentahydrate² and barium 5-amino-1*H*-tetrazolate tetrahydrate³ were synthesized as previously reported. Barium picratate hexahydrate⁴ was synthesized by a literature modified procedure as described below. ¹H, ¹³C, ³⁵Cl and ^{14/15}N NMR spectra were recorded on a DRX400 Bruker instrument. The spectra were measured in DMSO-d₆ at 25 °C unless otherwise specified. The chemical shifts are given relative to tetramethylsilane (¹H, ¹³C), sodium chloride (³⁵Cl) or ammonia (¹⁵N) as external standards. Infrared (IR) spectra were recorded at room temperature on a Perkin-Elmer Spectrum instrument equipped with a Universal ATR sampling accessory. Raman spectra were recorded on a Perkin-Elmer Spectrum 2000R NIR FT-Raman instrument equipped with a Nd:YAG laser (1064 nm). IR intensities are given in parentheses as vw = very weak, w = weak, m = medium, s = strong and vs = very strong. Raman activities are reported in percentages relative to the most intense peak and are given in parentheses. Elemental analyses were performed with a Netsch Simultaneous Thermal Analyzer STA 429. Melting points were determined by differential scanning calorimetry (SETARAM DSC131 instrument, calibrated with standard pure indium and zinc). Measurements were performed at a heating rate of $\beta = 5 \text{ °C min}^{-1}$ in closed aluminium containers with a hole (1 mm) on the top for gas release with a nitrogen flow of 20 mL min⁻¹. The reference sample was a closed aluminium container.

Synthesis of (CH₃)₂N(CH₂Cl)NH₂]Cl (**1**)

Method 1 (modified from ref. ¹²): 1,1-dimethylhydrazine (0.36 mL, 4.73 mmol) was dissolved in dichloromethane (5.0 mL, 78.12 mmol) under an inert atmosphere of nitrogen to give a colorless solution, which was stirred at room temperature for 38 h. After this time, a colorless solid had formed. The solvent was then decanted and the remaining solid was washed with fresh dichloromethane and dried under high-vacuum (0.512 g, 75%). The pure solid is hygroscopic.

Method 2 (large scale procedure): 1,1-dimethylhydrazine (15.0 mL, 197.08 mmol) was loaded into a 250 mL Schlenk flask containing dichloromethane (150.0 mL, 2.344 mol). Single crystals of **1** precipitated upon stirring overnight (18.052 g, 63%). ρ (X-ray) = 1.163 g cm⁻³; C₃H₈N₂Cl₂ (MW = 143.01 g mol⁻¹, calc./found): C 25.19 / 25.02, H 5.64 / 5.51, N 19.59 / 19.36; DSC (5 °C min⁻¹): 108–109 °C (m.p.), 158 °C (rash dec.); m/z (ESI⁺, 70 eV, >5%): 60.0(7), 75(10),

109(100, C⁺), 111(34), 129.1(5), 131.1(7), 252.9(100, [C₂Cl]⁺), 398.8(36, [C₃Cl₂]⁺), 544.8(46, [C₄Cl₃]⁺), 654.9(33), 688.8(100, [C₅Cl₄]⁺), 800.7(24), 832.7(65, [C₆Cl₅]⁺); ¹H NMR (DMSO-d₆, 400.18 MHz, TMS) δ/ppm: 3.40 (6 H, s, -CH₃), 5.62 (2 H, s, -CH₂Cl), 6.66 (2 H, s(br), -NH₂); ¹³C [¹H] NMR (DMSO-d₆, 100.52 MHz, TMS) δ/ppm: 71.60 (1 C, -CH₂Cl), 53.16 (2 C, N-CH₃); ³⁵Cl NMR (DMSO-d₆, 49.03 MHz, NaCl) δ/ppm: 70.4 (Cl⁻); Raman $\tilde{\nu}$ /cm⁻¹ (rel. int.): 3168(7), 3059(47), 3032(98), 3022(60), 3007(51), 2963(45), 2939(51), 2882(12), 2833(6), 1451(15), 1350(3), 1304(4), 1249(3), 1162(2), 1102(3), 980(11), 918(10), 892(16), 807(12), 739(100), 502(2), 477(6), 439(11), 368(12), 245(5); IR $\tilde{\nu}$ /cm⁻¹ (golden gate, rel. int.): 3155(m) 3099(m) 3019(s) 3007(s) 2884(w) 2686(w) 2169(w) 1780(w) 1694(w) 1631(m) 1468(m) 1447(w) 1430(w) 1398(w) 1351(m) 1305(w) 1242(m) 1159(m) 1118(m) 1099(m) 1009(w) 981(w) 922(m) 890(s) 798(s) 738(w) 619(w) 590(w) 569(w).

Synthesis of (CH₃)₂N(CH₂Cl)NH₂]₂[SO₄] (6)

1 (4.198 g, 28.95 mmol) and silver sulfate (4.559 g, 14.48 mmol) were loaded in a Schlenk flask filled with dry nitrogen and distilled water (25 mL) was added giving a suspension, which was stirred for 4 h at room temperature and under the exclusion of light. After this time, a pale yellow solution had formed and the insoluble silver chloride was filtered and washed thoroughly with distilled water. The solvent was then stripped under reduced pressure leaving behind a colorless semicrystalline solid (4.243 g, 93 %). Single crystals of the compound suitable for X-ray analysis formed upon slow evaporation of a methanolic solution. ρ (X-ray) = 1.549 g cm⁻³; C₆H₂₀Cl₂N₄O₄S (MW = 315.22 g mol⁻¹, calc./found): C 22.86 / 22.56, H 6.40 / 6.49, N 17.77 / 17.42; DSC (5 °C min⁻¹): 62.0 °C (m.p.), >180 °C (dec.); m/z (+c ESI): 109.1 (100, [Cat⁺]), 254.9 (29, [2 CatA]), 315.9 (6, [M + H⁺]), 422.9 (91, [Cat₃A]), 738.9 (36, [Cat₅A₂]); m/z (-c ESI): 97.0 (51, [A²⁻ + H⁺]), 726.8 (100, [Cat₄A₃ + H⁺]), 932.8 (48, [Cat₆A₄ + H⁺]); ¹H NMR (DMSO-d₆, 400.18 MHz, TMS) δ/ppm: 3.31 (6 H, s, -CH₃), 5.37 (2 H, s, -CH₂Cl), 6.28 (2 H, s(br), -NH₂); ¹³C [¹H] NMR (DMSO-d₆, 100.52 MHz, TMS) δ/ppm: 72.28 (2 C, -CH₂Cl), 53.55 (4 C, N-CH₃); Raman $\tilde{\nu}$ /cm⁻¹ (rel. int.): 3087(10), 3050(35), 3033(62), 2975(48), 2791(3), 1456(15), 1439(7), 1400(2), 1356(3), 1316(3), 1232(2), 1124(4), 1015(5), 970(100), 926(6), 896(9), 799(11), 742(94), 615(3), 503(4), 482(2), 449(5), 436(6), 389(2), 367(9), 312(1), 280(2), 240(4); IR $\tilde{\nu}$ /cm⁻¹ (golden gate, rel. int.): 3388(w) 3208(w) 3032(m) 1635(w) 1476(w) 1448(w) 1400(w) 1353(w) 1312(w) 1252(w) 1165(w) 1131(m) 1105(m) 10 vfg45(s) 1017(m) 968(w) 929(w) 893(m) 789(m) 738(w) 705(w) 673(w) 652(w) 609(vs) 538(w) 495(w) 478(w).

Synthesis of Silver Azide (AgN₃)

Silver nitrate (0.849 g, 5.00 mmol) was dissolved in distilled water (10 mL) and a solution of sodium azide (0.325 g, 5.00 mmol) in the same solvent (10 mL) was added slowly under slow

stirring. After the addition was finished, the reaction mixture was covered with aluminium paper and the reaction was left to reach completion. After ca. 20 min, the insoluble (**highly sensitive!**) silver azide was filtered by gravity, washed with water and acetone and left to air dry overnight. After this time, the silver azide was loaded into a plastic flask and stored in an explosive cage under the exclusion of light previous to immediate use (0.710 g, 95%).

Synthesis of Barium Picrate Tetrahydrate ($\text{Ba}[(\text{NO}_2)_3\text{Ph-O}]_2 \cdot 4\text{H}_2\text{O}$)

Picric acid (2.300 g, 10.04 mmol) was loaded in a 100 mL plastic beaker and dissolved in distilled water (55 mL) at ca. 90 °C (a small amount of picric acid remained undissolved). At this point 98% barium hydroxide octahydrate (1.616 g, 5.02 mmol) was added portion-wise as the neat solid resulting in the formation of a clear bright orange solution, which was further stirred at this temperature for 30 min. A crystalline solid precipitated upon cooling to room temperature that was recrystallized twice from hot water (2.360 g, 71%) and used for the synthesis of the picrate salt in this work. Single crystals of the hexahydrate suitable for X-ray analysis formed upon recrystallization from hot water. $\text{C}_{12}\text{H}_{12}\text{N}_6\text{O}_{18}\text{Ba}$ (MW = 665.58 g mol⁻¹, calc./found): C 21.65 / 21.79, H 1.81 / 1.76, N 12.62 / 12.46; DSC (5 °C min⁻¹): 35–45, 45–75, 75–90 and 125–150 °C (water loss), ≥315 °C (EX. dec.); m/z (+c ESI): 366.0 (61, [CatA]⁺), 959.7 (100, [Cat₂A₃]⁺), 1553.2 (25, [Cat₃A₅]⁺); m/z (-c ESI): 228.1 (34, [A]⁻), 478.7 (3, [A₂Na]⁻), 723.9 (24), 821.8 (53, [A₃Cat]⁻), 974.7 (100), 1415.5 (70, [A₅Cat₂]⁻); ¹H NMR (DMSO-d₆, 400.18 MHz, TMS) δ/ppm: 8.59 (4 H, s, H-Ar), 3.50 (8 H, s, H₂O); ¹³C [¹H] NMR (DMSO-d₆, 100.52 MHz, TMS) δ/ppm: 160.86 (1 C, C1), 141.81 (2 C, C2), 125.26 (2 C, C3), 124.42 (1 C, C4); Raman $\tilde{\nu}$ /cm⁻¹ (rel. int.): 3077(2), 1556(21), 1521(3), 1492(15), 1370(41), 1347(61), 1322(100), 1289(22), 1168(7), 1085(4), 945(15), 916(6), 827(35), 788(2), 750(4), 705(5), 546(2), 521(1), 366(1), 335(5), 162(6); IR $\tilde{\nu}$ /cm⁻¹ (golden gate, rel. int.): 3500(w) 3075(w) 1629(m) 1609(m) 1552(s) 1514(m) 1487(m) 1431(w) 1366(m) 1329(s) 1269(s) 1165(m) 1085(m) 934(w) 915(m) 838(w) 820(w) 795(w) 787(m) 744(m) 712(m) 702(m) 540(w) 499(w) 474(w).

X-ray Crystal Structure Discussion

An Oxford Diffraction Xcalibur 3 diffractometer equipped with a CCD detector using the CrysAlis Pro software was used for the measurements and data reduction.⁵ All data were collected using graphite-monochromated Mo-K_α radiation (λ = 0.71073 Å). The structures were solved by direct methods and refined by means of full-matrix least-squares procedures using WinGX and the available software in the package.^{6–9} Finally, the structures were checked using PLATON.¹⁰ The absorption corrections were performed using a SCALE3 ABSPACK multi-scan method.¹¹ All non-hydrogen atoms were refined anisotropically, whereas the hydrogen atoms were located from difference Fourier electron density maps and refined isotropically.

Table 3 contains data for the crystal structure solution and refinement for compounds **3**, **6**, **7**, **8** and $\text{Ba}[(\text{NO}_2)_3\text{Ph-O}]_2 \cdot 6\text{H}_2\text{O}$. Table 4 collects selected bond distances and angles for the $[(\text{CH}_3)_2\text{N}(\text{CH}_2\text{Cl})\text{NH}_2]^+$ cation and comparison with the optimized values by density functional theory calculations using B3LYP/6-311+G(d,p) levels of theory. Lastly, the hydrogen-bonding geometry of all compounds and the coordination around the Ba^{2+} cations in $\text{Ba}[(\text{NO}_2)_3\text{Ph-O}]_2 \cdot 6\text{H}_2\text{O}$ are summarized in Tables 2 and 3 from the supporting information. Further information concerning the crystal structure determination (excluding structure factors) in CIF format is available from the Cambridge Crystallographic Data Centre.¹³

Compounds **3**, **7** and $(\text{Ba}[(\text{NO}_2)_3\text{Ph-O}]_2 \cdot 6\text{H}_2\text{O})$ have triclinic cells of the space group $P-1$ (Table 3), whereas **6** and **8** crystallize in monoclinic cells in the space group C_2/c . In Table 4 the computed bond lengths and angles are listed following the corresponding data obtained for single crystals of salts **3**, **6**, **7** and **8**. The optimized gas phase structure of the cation is essentially the same as that observed from experimental data, i.e., the computed bond lengths and angles are consistent with the X-ray data. The slightly longer calculated values can be attributed to the lack of molecular packing in the gas phase. The average angle around the central nitrogen atom (N3) is close to the ideal tetrahedral angle. The N3-N6 bond distance (ca. 1.45 Å) is in keeping with the N-N distance found in 1,1-dimethylhydrazine¹⁴ and is typical for N-N single bonds.¹⁵ The distances between the amino hydrogen atoms of the $[(\text{CH}_3)_2\text{N}(\text{CH}_2\text{Cl})\text{NH}_2]^+$ cations and the anions in all compounds are shorter than the minimum N-N and N-O non-bonded distance, indicating that both amino hydrogen atoms form hydrogen-bonds to the anion (Table 5).

The sulphur atom of the $[\text{SO}_4]^{2-}$ anion in $[(\text{CH}_3)_2\text{N}(\text{CH}_2\text{Cl})\text{NH}_2]_2[\text{SO}_4]$ (**6**) lies on a symmetry plane so that half of the formula unit is generated by symmetry (symmetry code: (i) $2-x, y, 0.5-z$). As introduced above, the geometry of the cation with the $-\text{CH}_2\text{Cl}$ group pointing in the opposite direction of the $\text{N}-\text{NH}_2$ moiety is reminiscent of that of $[\text{Me}_2\text{N}(\text{CH}_2\text{Cl})\text{NH}_2]\text{Cl}$ (**1**).

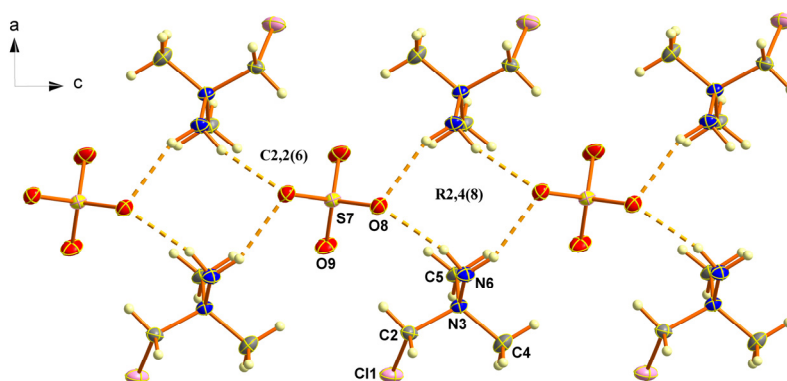


Fig. 1 Hydrogen-bonding in the crystal structure of $[(\text{CH}_3)_2\text{N}(\text{CH}_2\text{Cl})\text{NH}_2]_2[\text{SO}_4]$ (**6**) with the labeling scheme (Diamond plot at 50% probability). The dashed lines represent hydrogen-bonding between the $[(\text{CH}_3)_2\text{N}(\text{CH}_2\text{Cl})\text{NH}_2]^+$ cations and the $[\text{SO}_4]^{2-}$ anions.

The $[\text{SO}_4]^{2-}$ anions have the expected tetrahedral geometry¹⁶ with two different S–O distances (S7–O8 and S7–O9). This can be attributed to the fact that O9 does not participate in the formation of classical hydrogen bonds (shortest contact: $\text{C2}\cdots\text{O9} = 3.203(7) \text{ \AA}$), whereas O8 forms two crystallographically independent hydrogen bonds (Table 5) and, in consequence, the S7–O8 distance is slightly elongated in comparison to the S7–O9 distance ($1.491(3) \text{ \AA}$ vs. $1.460(3) \text{ \AA}$). These two hydrogen-bonds form dimeric interactions of the type **D1,1(2)** [**D2,2(5)**] (primary level) and combine at the secondary level to form ring patterns of the type **R2,4(8)** with **C2,2(6)** infinite chains along the *c*-axis, which connect the dimer pairs depicted in Fig. 1). These latter graph-sets are analogous to those of the perchlorate salt (see discussion above), as might be expected from the strong similarities in the geometry between the $[\text{SO}_4]^{2-}$ and the $[\text{ClO}_4]^-$ anions. In contrast to the perchlorate salt, however, these dimer pairs interact only *via* unclassical hydrogen-bonds along the *a*- and *b*-directions (Fig. 2).

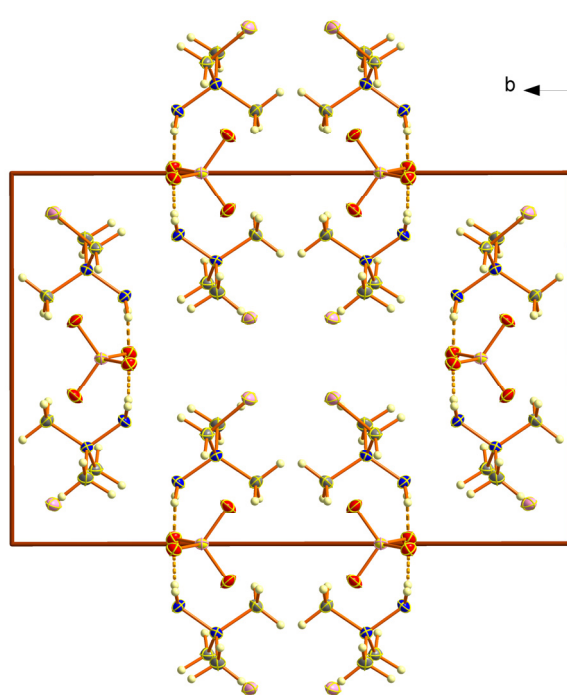


Fig. 2 Unit cell of $[(\text{CH}_3)_2\text{N}(\text{CH}_2\text{Cl})\text{NH}_2]_2[\text{SO}_4]$ (**6**, view along the *c*-axis) with hydrogen-bonding (dotted lines).

Fig. 3 shows the asymmetric unit of $[(\text{CH}_3)_2\text{N}(\text{CH}_2\text{Cl})\text{NH}_2]_2[\text{N}_4\text{C}=\text{N}=\text{N}=\text{CN}_4]^{2-}$ (**7**), which is made up of one $[\text{N}_4\text{C}=\text{N}=\text{N}=\text{CN}_4]^{2-}$ anion and two crystallographically independent $[(\text{CH}_3)_2\text{N}(\text{CH}_2\text{Cl})\text{NH}_2]^+$ cations. As pointed out in the introductory discussion of this section, the orientation of the $-\text{CH}_2\text{Cl}$ group in both cations is different. While one of the two cations has the $-\text{CH}_2\text{Cl}$ and $\text{N}-\text{NH}_2$ moieties pointing in opposite directions, the other cation shows a rotation of the N3–N6 bond and in analogy to the perchlorate salt, it forms an intramolecular hydrogen-bond ($\text{N6}\cdots\text{Cl1} = 3.134(2) \text{ \AA}$), which describes an **S(5)** ring graph-set.

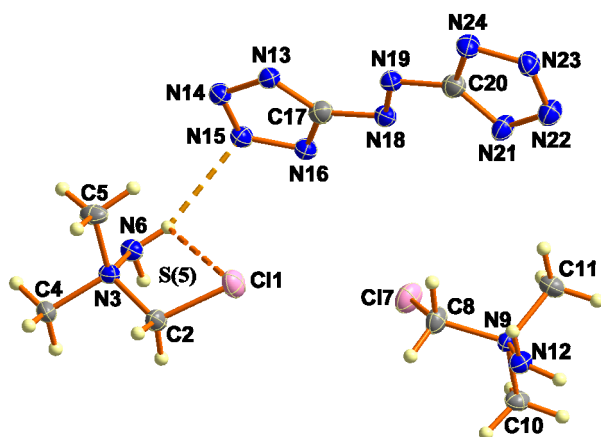


Fig. 3 Asymmetric unit of $[(\text{CH}_3)_2\text{N}(\text{CH}_2\text{Cl})\text{NH}_2]_2[\text{N}_4\text{C}-\text{N}=\text{N}-\text{CN}_4]$ (**7**) with the labeling scheme (Diamond plot at 50% probability). The dashed lines represent hydrogen-bonding.

The $[\text{N}_4\text{C}-\text{N}=\text{N}-\text{CN}_4]^{2-}$ anions in $[(\text{CH}_3)_2\text{N}(\text{CH}_2\text{Cl})\text{NH}_2]_2[\text{N}_4\text{C}-\text{N}=\text{N}-\text{CN}_4]$ (**7**) form planar layers with an interlayer distance $\text{N21}-\text{N23}^{\text{viii}} = 3.590(3)$ Å (symmetry code: (viii) $2-x, 1-y, -z$). Like for the remainder of the salts of the $[(\text{CH}_3)_2\text{N}(\text{CH}_2\text{Cl})\text{NH}_2]^+$ cation in this work, there exist many unclassical hydrogen-bonds in the structure of the compound (Table 5), the most important one between one of the methyl group hydrogen atoms in the cation and one ring nitrogen of the anion ($\text{C11}\cdots\text{N21}^{\text{v}} = 3.269(3)$ Å; symmetry code: (v) $1-x, 1-y, -z$). Fig. 4 shows a view of the classical hydrogen-bonding around the $[\text{N}_4\text{C}-\text{N}=\text{N}-\text{CN}_4]^{2-}$ anion. Every anion is acceptor of four classical hydrogen-bonds by four cations. These hydrogen-bonds make dimeric interactions of the type **D1,1(2)** at the unitary level, whereas at the secondary level, there exists finite chain patterns with the descriptor **D2,2(X)** ($X = 4, 5, 8, 9$) and **R4,4(X)** ($X = 10, 20$) ring graph-sets, but no infinite chain networks. The **R4,4(10)** motifs are formed by the interaction of two tetrazole rings with two cations ($\text{N6}\cdots\text{N15} = 3.213(3)$ Å and $\text{N6}\cdots\text{N16}^{\text{vii}} = 3.026(3)$ Å; symmetry code: (vii) $1-x, -y, 1-z$) and the larger **R4,4(20)** involve hydrogen-bonding between four tetrazole rings and two cations ($\text{N12}\cdots\text{N24}^{\text{iii}} = 2.989(3)$ Å and $\text{N12}\cdots\text{N14}^{\text{vi}} = 3.074(3)$ Å; symmetry codes: (iii) $2-x, 1-y, -z$; (vi) $x, y, -1+z$).

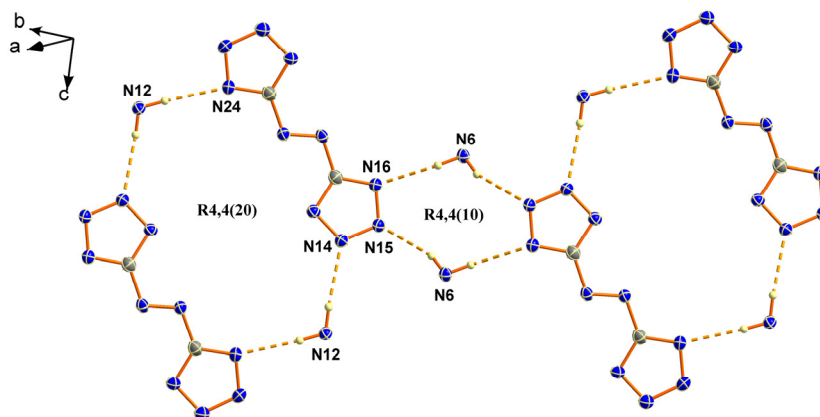


Fig. 4 Ring hydrogen-bonding (dotted lines) networks in the crystal structure of $[(\text{CH}_3)_2\text{N}(\text{CH}_2\text{Cl})\text{NH}_2]_2[\text{N}_4\text{C}-\text{N}=\text{N}-\text{CN}_4]$ (**7**, for simplification purposes only the $-\text{NH}_2$ groups of the $[(\text{CH}_3)_2\text{N}(\text{CH}_2\text{Cl})\text{NH}_2]^+$ cations are represented).

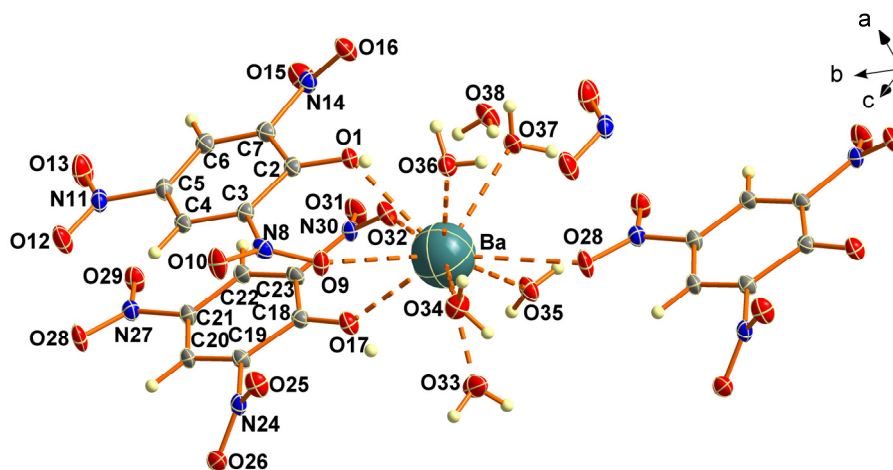


Fig. 5 Packing around the Ba^{2+} cations in the crystal structure of $\text{Ba}[(\text{NO}_2)_3\text{Ph-O}]_2 \cdot 6\text{H}_2\text{O}$ and labelling scheme (Diamond ellipsoids at 50 % probability). Dashed lines indicate coordination to the Ba^{2+} cations.

Barium picrate was used for the synthesis of $[(\text{CH}_3)_2\text{N}(\text{CH}_2\text{Cl})\text{NH}_2][(\text{NO}_2)_3\text{Ph-O}]$ (**8**). After recrystallization from hot water of the tetrahydrate, single crystals of the hexahydrate salt ($\text{Ba}[(\text{NO}_2)_3\text{Ph-O}]_2 \cdot 6\text{H}_2\text{O}$) formed. The asymmetric unit of the compound is represented in Fig. 5. The Ba^{2+} cations have a coordination number of 10 with Ba–O distances which vary within a relatively narrow range (ca. 2.7–3.1 Å, Table 6) and are slightly shorter than, for example, for barium 5,5'-hydrazine-1,2-diylbis(1*H*-tetrazolate) pentahydrate¹⁷ or barium 5,5'-azobistetrazolate pentahydrate.¹⁸ The coordination environment of the Ba^{2+} cations is completed by interactions to the phenolate oxygen atoms of the picrate anions (O1 and O17), to the nitro-group oxygen atoms of the picrate anions (O19, O28 and O32) and to the oxygen atoms of all molecules of crystal water except for O38 (Ba–O38 = 4.673(3) Å), which is only involved in the formation of hydrogen-bonding. The $\text{Ba}[(\text{NO}_2)_3\text{Ph-O}]_2 \cdot 6\text{H}_2\text{O}$ units are connected by coordination (O28ⁱ–Ba = 3.002(3) Å; symmetry code: (i) $x, 1+y, z$) and form infinite chains along a direction approximately parallel to the *b*-axis (Fig. 5). Additionally, the aromatic rings of the two picrate anions interact *via* π -stacking. The $-\text{NO}_2$ groups of the picrate anions are tilted off the plane of the aromatic ring. For one of the two crystallographically independent anions, the *p*- NO_2 group is essentially coplanar to the ring (dihedral angle C6–C5–N11–O13 = ca. 2°), whereas the *o*- NO_2 groups are tilted by ca. 32°. For the other anion, the *p*- NO_2 is tilted ca. 12°, whereas the two *o*- NO_2 groups are twisted ca. 23 and 44°. The difference in the tilt angle of the $-\text{NO}_2$ groups is probably related to packing effects and hydrogen bonding.¹⁹

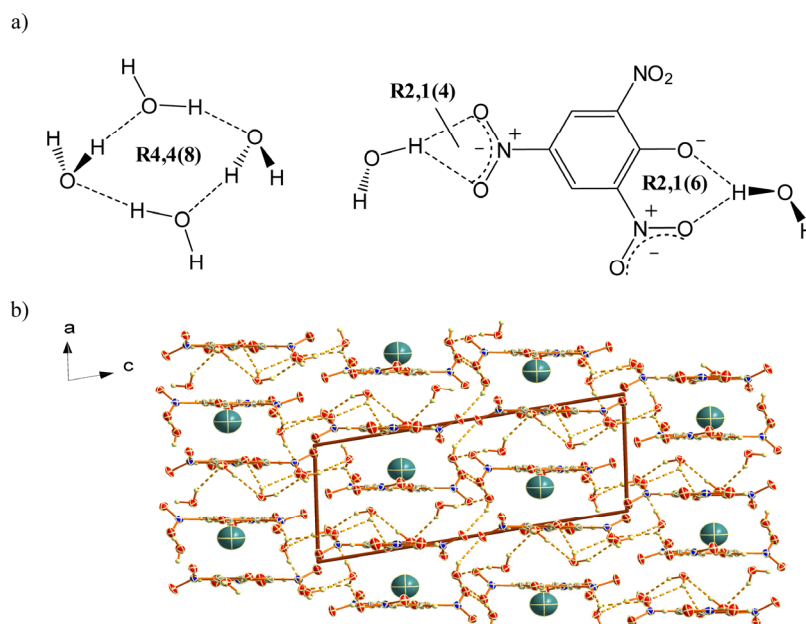


Fig. 6 a) Schematic representation of the ring graph-sets found in the crystal structure of $\text{Ba}[(\text{NO}_2)_3\text{Ph-O}]_2 \cdot 6\text{H}_2\text{O}$ and b) unit cell of $\text{Ba}[(\text{NO}_2)_3\text{Ph-O}]_2 \cdot 6\text{H}_2\text{O}$ (view along the b -axis) with hydrogen-bonding (dotted lines). The coordination around the Ba^{2+} cations has been omitted for clarity purposes.

Fig. 6b shows a representation of the unit cell of the compound with the hydrogen-bonding (dotted lines). The compound forms, considering only the benzene rings, planar layers on the bc -plane with infinite π -stacks of anions along the a -axis. The layers are connected by extensive hydrogen-bonding to water molecules, which form a total of 14 medium-to-strong hydrogen bonds. The extensive hydrogen-bonding found in the structure of the compound can be better understood by looking at the hydrogen-bonding graph-sets. At the primary level, each one of the 14 hydrogen bonds is only involved in **D1,1(2)** dimeric interactions. The secondary level is highly dominated by dimeric interactions of the type **D1,2(3)**, **D2,1(3)** and **D2,2(X)** ($X = 4, 5, 7, 9$) and additionally some ring graph-sets with the descriptor **R2,1(X)** ($X = 4, 6$) and **R4,4(8)** are also found. No infinite chain interactions of the type **Ca,b(X)** were identified by the program *RPLUTO*. Fig. 6a gives an schematic representation of the ring hydrogen-bonding networks found in the crystal structure. The **R4,4(8)** motifs are formed by interaction between four molecules of crystal water ($\text{O38} \cdots \text{O37} = 2.821(5) \text{ \AA}$ and $\text{O37} \cdots \text{O38}^{\text{vii}} = 2.798(5) \text{ \AA}$; symmetry code: (vii) $2-x, -y, -z$), whereas the **R2,1(4)** and **R2,1(6)** networks are formed by interaction of one molecule of crystal water with the p - NO_2 group ($\text{O36} \cdots \text{O12}^{\text{v}} = 2.908(5) \text{ \AA}$ and $\text{O36} \cdots \text{O13}^{\text{v}} = 3.168(5) \text{ \AA}$; symmetry code: (v) $x, -1+y, z$) and with one of the o - NO_2 groups and the phenolate oxygen atom ($\text{O35} \cdots \text{O1}^{\text{i}} = 2.741(5) \text{ \AA}$ and $\text{O35} \cdots \text{O16}^{\text{i}} = 3.044(5) \text{ \AA}$; symmetry code: (i) $-1+x, y, z$), respectively.

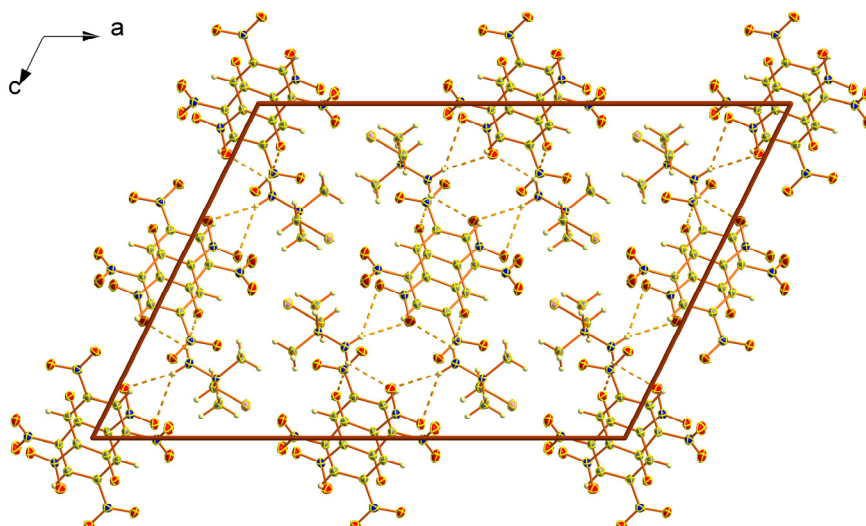


Fig. 7 Unit cell of $[(\text{CH}_3)_2\text{N}(\text{CH}_2\text{Cl})\text{NH}_2][(\text{NO}_2)_3\text{Ph-O}]$ (**8**, view along the b -axis) with hydrogen-bonding (dotted lines).

In $[(\text{CH}_3)_2\text{N}(\text{CH}_2\text{Cl})\text{NH}_2][(\text{NO}_2)_3\text{Ph-O}]$ (**8**), one of the $-\text{NO}_2$ groups of the picrate anion is nearly coplanar to the benzene ring ($\text{C}8-\text{C}9-\text{N}14-\text{O}15 = 0.2^\circ$), one is slightly tilted ($\text{C}10-\text{C}11-\text{N}17-\text{O}18 = 9.0^\circ$) and one is more significantly off the aromatic plane ($\text{C}12-\text{C}13-\text{N}20-\text{O}22 = 32.3^\circ$). Fig. 7 shows a view of the unit cell of the compound. The two hydrogen atoms of the $\text{N}-\text{NH}_2$ moiety in the cation are involved in two hydrogen bonds each forming dimer pairs that interact with other dimer pairs through, at least, one of the 9 unclassical $\text{C}\cdots\text{O}$ hydrogen bonds summarized in Table 5 and that are common for picrate salts.⁷

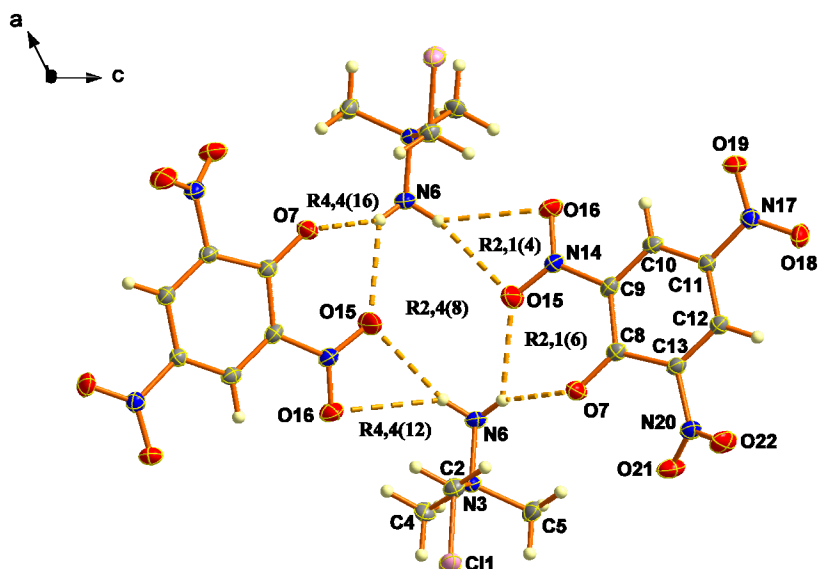


Fig. 8 Hydrogen-bonding in the crystal structure of $[(\text{CH}_3)_2\text{N}(\text{CH}_2\text{Cl})\text{NH}_2][(\text{NO}_2)_3\text{Ph-O}]$ (**8**) with the labeling scheme (Diamond plot at 50% probability). The dashed lines represents hydrogen-bonding between the $[(\text{CH}_3)_2\text{N}(\text{CH}_2\text{Cl})\text{NH}_2]^+$ cations and the $[(\text{NO}_2)_3\text{Ph-O}]^-$ anions.

The structure of one of these hydrogen-bonded dimer pairs is represented in Fig. 8. The first level hydrogen-bonding network of the compound is made up of four **D1,1(2)** dimeric interactions, whereas at the secondary level, ring graph-sets of the type **R2,1(X)** ($X = 4, 6$), **R2,4(8)** and **R4,4(X)** ($X = 12, 16$) are formed. Similarly to what is found for $[(\text{CH}_3)_2\text{N}(\text{CH}_2\text{Cl})\text{NH}_2]_2[\text{N}_4\text{C}=\text{N}=\text{N}-\text{CN}_4]$ (**6**), no infinite chain motifs can be identified. These hydrogen-bonding networks are also depicted in Fig. 8. For example, the **R4,4(12)** graph-sets are formed by the interaction of two cations and two anions ($\text{N6}\cdots\text{O16}^{\text{i}} = 3.309(3) \text{ \AA}$ and $\text{N6}\cdots\text{O15}^{\text{iii}} = 2.917(3) \text{ \AA}$; symmetry codes: (i) $x, 1-y, 0.5+z$; (iii) $1-x, 1-y, 1-z$) whereas the combination of $\text{N6}\cdots\text{O16}^{\text{i}}$ and $\text{N6}\cdots\text{O7}^{\text{iii}} = 2.841(3) \text{ \AA}$ results in the formation of the larger **R4,4(16)** ring motifs.

Table 1 Calculated (scaled) and measured IR and Raman frequencies with intensity (IR) and activity (Raman) values for the $[(\text{CH}_3)_2\text{N}(\text{CH}_2\text{Cl})\text{NH}_2]^+$ cation.

	ν_{scal} (cm^{-1}) ^a	$I_{\text{calc}}/A_{\text{calc}}$ IR/Raman ^b	ν_{meas} (IR, cm^{-1}) ^c	ν_{meas} (Raman, cm^{-1}) ^d	Mode Assignment ^e
1	103	4/1			$\omega(\text{C-H})$
2	217	2/-			$\omega(\text{C-H}) + \omega(\text{N-H})$
3	224	21/1			$\omega(\text{C-H}) + \gamma(\text{N-H})$
4	256	21/1		245(5)	$\omega(\text{C-H}) + \gamma(\text{N-H})$
5	267	12/-			$\omega(\text{C-H}) + \omega(\text{N-H})$
6	339	-1/2			$\delta(\text{C-N-N}) + \delta(\text{C-N-C})$
7	347	1/1		360(5)	$\omega(\text{C-H})$
8	413	3/1			$\delta(\text{C-N-N}) + \delta(\text{C-N-C})$
9	446	6/1		440(5)	$\tau(\text{C-H}) + \tau(\text{N-H})$
10	485	3/2		480(5)	$\delta(\text{C-N-N}) + \delta(\text{C-N-C})$
11	693	-/20	565(w)		$\nu_s(\text{N-C})$
12	785	65/2	740(m)	740(60)	$\nu(\text{N-N}) + \nu(\text{C-Cl})$
13	813	60/5	800(m)	805(5)	$\omega(\text{N-H})$
14	866	20/5			$\omega(\text{C-H})$
15	913	13/5	890(m)	890(10)	$\omega(\text{N-H}) + \gamma(\text{C-H})$
16	961	4/1	940(m)	970(10)	$\omega(\text{C-H}) + \tau(\text{C-H})$
17	1002	60/5			$\omega(\text{N-H}) + \tau(\text{C-H})$
18	1076	-/-	1045(w)		$\tau(\text{C-H}) + \tau(\text{N-H})$
19	1098	2/1	1095(w)	1120(1)	$\tau(\text{C-H}) + \tau(\text{N-H})$
20	1180	2/3	1165(w)	1160(1)	$\tau(\text{C-H}) + \tau(\text{N-H})$
21	1201	4/1		1200(1)	$\tau(\text{C-H}) + \tau(\text{N-H})$
22	1251	1/3	1245(w)	1250(5)	$\tau(\text{C-H}) + \tau(\text{N-H})$
23	1306	14/2	1300(w)	1295(5)	$\gamma(\text{C-H}) + \gamma(\text{N-H})$
24	1352	6/1	1340(w)		$\gamma(\text{C-H}) + \gamma(\text{N-H})$
25	1387	5/1			$\gamma(\text{C-H})$
26	1405	6/3	1390(w)		$\gamma(\text{C-H})$
27	1418	5/7			$\delta(\text{C-H})$
28	1421	1/10			$\delta(\text{C-H})$
29	1429	6/3	1430(w)		$\delta(\text{C-H})$
30	1448	33/1	1450(m)	1450(10)	$\delta(\text{C-H})$
31	1454	42/2	1470(m)		$\delta(\text{C-H})$
32	1612	55/2	1620(m)		$\delta(\text{N-H})$
33	2951	-/45		2880(30)	$\nu_s(\text{C-H})$
34	2959	1/139	2990(w)	2980(60)	$\nu_s(\text{C-H})$
35	2991	3/84	3030(m)	3050(30)	$\nu_s(\text{C-H})$
36	3041	-/25			$\nu_s(\text{C-H}) + \nu_{as}(\text{C-H})$
37	3047	-/30			$\nu_s(\text{C-H}) + \nu_{as}(\text{C-H})$
38	3053	-/40			$\nu_{as}(\text{C-H})$
39	3066	1/19			$\nu_{as}(\text{C-H})$
40	3069	3/48			$\nu_{as}(\text{C-H})$
41	3332	26/94	3180(m)	3170(5)	$\nu_s(\text{N-H})$
42	3420	30/38	3275(m)		$\nu_{as}(\text{N-H})$

^a Calculated frequencies (B3LYP/6-311+G(d,p))²⁰ scaled by 0.9613;²¹ ^b Calculated IR intensities and Raman activities. ^c Experimental IR frequencies and intensities in () brackets. ^d Experimental Raman frequencies and activities in () brackets. ^e Approximate description of vibrational modes: ν = stretching, δ = in-plane bending, γ = out-of-plane bending, ω = in-plane rocking, τ = torsion; as = asymmetric and s = symmetric.

Table 2 ^1H , ^{13}C and ^{15}N NMR chemical shifts (ppm) for the $[(\text{CH}_3)_2\text{N}(\text{CH}_2\text{Cl})\text{NH}_2]^+$ cation in compounds **1–9**.^a

	^1H NMR			^{13}C NMR		$^{14/15}\text{N}$ NMR ^b	
	–CH ₃	–CH ₂ Cl	–NH ₂	–CH ₃	–CH ₂ Cl	–N(CH ₃) ₂	–NH ₂
$[(\text{CH}_3)_2\text{N}(\text{CH}_2\text{Cl})\text{NH}_2]\text{Cl}$ (1)	3.40	5.62	6.66	53.16	71.60		
$[(\text{CH}_3)_2\text{N}(\text{CH}_2\text{Cl})\text{NH}_2][\text{NO}_3]$ (2)	3.31	5.34	6.22	53.15	71.57	+84.6 (s)	+115.6 ($^1J = 66.7$)
$[(\text{CH}_3)_2\text{N}(\text{CH}_2\text{Cl})\text{NH}_2][\text{ClO}_4]$ (3)	3.30	5.33	6.21	53.18	71.60		
$[(\text{CH}_3)_2\text{N}(\text{CH}_2\text{Cl})\text{NH}_2][\text{N}_3]$ (4)	3.33	5.42	6.42	53.43	72.09	+85 (s(br))	-
$[(\text{CH}_3)_2\text{N}(\text{CH}_2\text{Cl})\text{NH}_2][\text{N}(\text{CN})_2]$ (5)	3.29	5.31	6.19	53.37	72.01		
$[(\text{CH}_3)_2\text{N}(\text{CH}_2\text{Cl})\text{NH}_2]_2[\text{SO}_4]$ (6)	3.31	5.37	6.28	53.55	72.28		
$[(\text{CH}_3)_2\text{N}(\text{CH}_2\text{Cl})\text{NH}_2]_2$ $[\text{N}_4\text{C-N=N-CN}_4]$ (7)	3.41	5.57	6.59	53.51	72.08		
$[(\text{CH}_3)_2\text{N}(\text{CH}_2\text{Cl})\text{NH}_2]$ $[(\text{NO}_2)_3\text{Ph-O}]$ (8)	3.33	5.40	6.32	53.56	72.27		
$[(\text{CH}_3)_2\text{N}(\text{CH}_2\text{Cl})\text{NH}_2]$ $[\text{H}_2\text{N-CN}_4]$ (9)	3.37	5.52	6.53	53.34	71.93		

^a in DMSO-*d*₆. ^b ^{15}N NMR for salt **2** and ^{14}N NMR for salt **4** (NH_3 as external standard; $\delta(\text{MeNO}_2) = \delta(\text{NH}_3) - 381$). One bond N–H coupling constant (1J) for compound **2** in Hz.

Table 3 Crystal structure solution and refinement for salts of the $[(\text{CH}_3)_2\text{N}(\text{CH}_2\text{Cl})\text{NH}_2]^+$ cation. $R_1 = \Sigma ||F_o| - |F_c|| / \Sigma |F_o|$; $R_w = [\Sigma (F_o^2 - F_c^2) / \Sigma w (F_o^2)]^{1/2}$; $w = [\sigma_c^2 (F_o^2) + (xP)^2 + yP]^{-1}$, $P = (F_o^2 - 2F_c^2) / 3$.

Parameter	3	6	7	8	BaPic ^a
CCDC No ^c	808540	808541	808542	808543	808544
Formula	C ₃ H ₁₀ Cl ₂ N ₂ O ₄	C ₆ H ₂₀ Cl ₂ N ₄ O ₄ S	C ₈ H ₂₀ Cl ₂ N ₁₄	C ₉ H ₁₂ N ₅ ClO ₇	C ₁₂ H ₁₆ N ₆ O ₂₀ Ba
<i>M</i> _r , g mol ⁻¹	209.03	315.22	383.24	337.69	701.63
<i>T</i> , K	100(2)	110(2)	110(2)	110(2)	110(2)
Cryst. descr.	Plate	Block	Block	Plate	Needle
Cryst. color	Colorless	Colorless	Yellow	Yellow	Yellow
Cryst. size	0.52x0.23x0.04	0.27x0.17x0.11	0.47x0.24x0.16	0.55x0.25x0.14	0.51x0.11x0.09
Cryst. syst.	Triclinic	Monoclinic	Triclinic	Monoclinic	Triclinic
space gr.	<i>P</i> -1	<i>C</i> 2/ <i>c</i>	<i>P</i> -1	<i>C</i> 2/ <i>c</i>	<i>P</i> -1
<i>a</i> , Å	5.983(1)	11.674(2)	8.851(1)	24.168(3)	6.641(1)
<i>b</i> , Å	7.502(1)	17.503(2)	8.872(1)	7.375(1)	11.588(1)
<i>c</i> , Å	9.335(1)	6.616(1)	11.529(1)	17.062(3)	15.033(1)
α , °	93.86(1)	90	80.98(1)	90	84.64(1)
β , °	101.21(1)	90.27(1)	83.47(1)	116.19(2)	80.07(1)
γ , °	91.13(1)	90	71.37(1)	90	86.80(1)
<i>V</i> , Å ³	409.8(1)	1351.8(3)	845.5(1)	1351.8(3)	1133.8(1)
<i>Z</i>	2	4	2	8	2
ρ , g cm ⁻³	1.694	1.549	1.521	1.644	2.055
μ , cm ⁻¹	6.99	0.64	0.41	0.32	1.86
<i>F</i> (000), e	216	664	404	1392	692
θ range / °	4.83–66.12	3.49–29.24	3.58–29.48	3.51–29.49	3.40–29.57
<i>hkl</i> range	–6 ≤ <i>h</i> ≤ 7 –8 ≤ <i>k</i> ≤ 8 –11 ≤ <i>l</i> ≤ 10	–15 ≤ <i>h</i> ≤ 15 –20 ≤ <i>k</i> ≤ 22 –8 ≤ <i>l</i> ≤ 8	–11 ≤ <i>h</i> ≤ 12 –12 ≤ <i>k</i> ≤ 12 –15 ≤ <i>l</i> ≤ 15	–30 ≤ <i>h</i> ≤ 29 –10 ≤ <i>k</i> ≤ 9 –23 ≤ <i>l</i> ≤ 22	–8 ≤ <i>h</i> ≤ 9 –15 ≤ <i>k</i> ≤ 15 –20 ≤ <i>l</i> ≤ 20
Refl. meas.	5330	2793	21463	10302	28809
Refl. unique	1418	1553	4325	3343	5785
<i>R</i> _{int} (data)	0.057(1418)	0.061(1553)	0.065(4325)	0.039(3343)	0.066(5785)
Restr./Par.	0/100	0/79	0/217	0/199	0/353
<i>R</i> (<i>F</i>)/ <i>wR</i> (<i>F</i> ²)	0.055/ (all refl.)	0.083/ 0.170	0.071/ 0.189	0.059/ 0.109	0.039/ 0.077
GoF (<i>F</i> ²)	1.008	0.985	1.005	0.995	0.997
$\Delta\rho_{\text{min}}$, e Å ⁻³	–0.55/ (max/min)	–0.73/ 0.98	–0.90/ 0.45	–0.57/ 0.57	–1.86/ 1.02

^a BaPic = Ba[(NO₂)₃Ph–O]₂*6H₂O.

Table 4 Experimental selected bond distances (in Å) and angles (in °) in the crystal structure of salts of the $[(\text{CH}_3)_2\text{N}(\text{CH}_2\text{Cl})\text{NH}_2]^+$ cation and comparison with the optimized parameters for the $[(\text{CH}_3)_2\text{N}(\text{CH}_2\text{Cl})\text{NH}_2]^+$ cation using DFT and MP2 methods.

Parameter ^a	3	6	7 (A)	7(B)	8	B3LYP ^b	MP2 ^c
C11–C2	1.769(2)	1.777(5)	1.758(2)	1.767(2)	1.767(2)	1.768	1.747
C2–N3	1.506(3)	1.498(6)	1.511(3)	1.503(3)	1.502(3)	1.529	1.520
N3–N6	1.458(3)	1.454(5)	1.445(2)	1.457(2)	1.455(2)	1.454	1.452
N3–C4	1.489(3)	1.499(6)	1.506(3)	1.501(3)	1.499(3)	1.509	1.502
N3–C5	1.506(3)	1.493(6)	1.494(3)	1.492(3)	1.497(3)	1.511	1.504
C11–C2–N3	110.5(2)	112.0(3)	111.6(1)	111.6(1)	112.4(2)	112.9	112.5
C2–N3–N6	113.6(2)	112.4(4)	114.8(2)	104.0(2)	108.4(2)	103.4	103.2
C2–N3–C4	111.8(2)	111.4(4)	111.7(2)	111.1(2)	112.0(2)	111.9	112.1
N6–N3–C4	108.0(2)	107.4(4)	106.5(2)	112.1(2)	107.1(2)	112.9	113.0
C2–N3–C5	107.6(2)	102.4(3)	106.7(2)	111.2(2)	111.3(2)	110.6	110.8
N6–N3–C5	106.5(2)	111.7(3)	107.5(2)	107.4(2)	107.2(2)	107.0	106.7
C4–N3–C5	109.0(2)	111.2(4)	109.2(2)	110.6(2)	110.2(2)	110.6	110.7

^a Symmetry code for **5**: (i) 2–x, y, 0.5–z; ^b B3LYP/6-31+G(d,p); ^c MP2/6-31++G(d,p).

Table 5 Geometry of medium to strong hydrogen bonds in the crystal structure of salts of the $[(\text{CH}_3)_2\text{N}(\text{CH}_2\text{Cl})\text{NH}_2]^+$ cation.

D-H...A	D-H (Å)	H...A (Å)	D...A (Å)	D-H...A (°)
3				
N6-H62...C11	0.8710(1)	2.820(4)	3.117(5)	101.8(1)
C2-H21...O10	0.9675(1)	2.455(5)	3.363(5)	156.2(1)
C4-H41...O8	0.9685(1)	2.507(5)	3.428(5)	158.7(1)
C2-H22...O9 ⁱ	0.9781(1)	2.537(5)	3.434(5)	152.4(1)
C5-H51...O9 ⁱ	0.9634(1)	2.567(5)	3.469(5)	155.8(1)
N6-H61...O8 ⁱ	0.8696(1)	2.213(4)	3.064(5)	166.0(1)
C5-H52...O8 ⁱⁱ	0.9491(1)	2.597(5)	3.469(5)	152.7(1)
N6-H62...O9 ⁱⁱⁱ	0.8709(1)	2.249(4)	3.101(5)	165.9(1)
6				
C2-H22...O9	0.9600(2)	2.300(4)	3.203(7)	156.0(1)
C2-H21...O8 ⁱ	0.9600(2)	2.350(3)	3.291(7)	165.3(1)
C4-H43...O9 ⁱⁱ	0.9500(2)	2.430(4)	3.293(7)	150.8(1)
N6-H62...O8	0.8600(2)	2.040(4)	2.870(7)	164.0(1)
N6-H61...O8 ⁱⁱⁱ	0.8600(2)	2.090(4)	2.907(7)	156.6(1)
7				
C11-H113...N21	0.969(1)	2.588(3)	3.379(3)	138.8(1)
C2-H21...N13 ⁱ	0.957(1)	2.597(3)	3.447(3)	148.1(1)
C4-H43...N19 ⁱ	0.954(1)	2.559(3)	3.400(3)	146.9(1)
C4-H52...N13 ⁱ	0.971(1)	2.521(3)	3.408(3)	151.8(1)
C4-H41...N22 ⁱⁱ	0.964(1)	2.476(3)	3.406(3)	161.7(1)
C8-H82...N23 ⁱⁱⁱ	0.952(1)	2.456(3)	3.331(3)	152.6(1)
C8-H81...N23 ^{iv}	0.954(1)	2.472(3)	3.402(3)	164.6(1)
C11-H112...N21 ^v	0.948(1)	2.499(3)	3.269(3)	138.2(1)
N6-H62...C11	0.860(1)	2.829(3)	3.134(2)	102.8(1)
N6-H62...N15	0.860(1)	2.386(3)	3.213(3)	161.4(1)
N12-H122...N24 ⁱⁱⁱ	0.872(1)	2.133(3)	2.989(3)	166.7(1)
N12-H121...N14 ^{vi}	0.870(1)	2.238(3)	3.074(3)	160.9(1)
N6-H61...N16 ^{vii}	0.876(1)	2.202(3)	3.026(3)	156.5(1)
8				
C2-H21...O18	0.950(1)	2.570(3)	3.242(3)	128.0(1)
C2-H21...O19	0.950(1)	2.460(3)	3.299(3)	147.0(1)
C2-H22...O16 ⁱ	0.970(1)	2.480(3)	3.336(3)	145.9(1)
C4-H43...O16 ⁱ	0.970(1)	2.460(3)	3.317(3)	147.9(1)
C5-H51...O19 ⁱⁱ	0.960(1)	2.380(3)	3.269(3)	152.9(1)
C5-H53...O7 ⁱⁱⁱ	0.950(1)	2.460(3)	3.223(3)	137.4(1)
C4-H42...O21 ^{iv}	0.980(1)	2.590(3)	3.255(3)	125.1(1)
C4-H42...O22 ^{iv}	0.980(1)	2.590(3)	3.558(3)	170.0(1)
C12-H121...O18 ^v	0.950(1)	2.430(3)	3.352(3)	162.2(1)
N6-H62...O15 ⁱ	0.870(1)	2.410(3)	3.259(3)	164.6(1)
N6-H62...O16 ⁱ	0.870(1)	2.570(3)	3.309(3)	142.7(1)
N6-H61...O7 ⁱⁱⁱ	0.860(1)	2.040(3)	2.841(3)	156.0(1)
N6-H61...O15 ⁱⁱⁱ	0.860(1)	2.300(3)	2.917(3)	128.5(1)
$\text{Ba}[(\text{NO}_2)_3\text{Ph-O}]_2 \cdot 6\text{H}_2\text{O}$				
O38-H382...O37	0.826(1)	2.013(4)	2.821(5)	165.5(1)
O33-H332...O36 ⁱ	0.820(1)	2.071(4)	2.832(5)	154.0(1)
O35-H352...O1 ⁱ	0.819(1)	2.011(4)	2.741(5)	148.1(1)
O35-H352...O16 ⁱ	0.819(1)	2.410(4)	3.044(5)	134.9(1)
O35-H351...O38 ⁱⁱ	0.810(1)	1.980(4)	2.746(5)	157.0(1)
O34-H342...O10 ⁱⁱⁱ	0.827(1)	2.128(4)	2.901(5)	155.2(1)
O33-H331...O35 ^{iv}	0.818(1)	2.117(4)	2.881(5)	155.1(1)
O34-H341...O25 ^{iv}	0.823(1)	2.196(4)	2.968(5)	156.3(1)
O36-H362...O12 ^v	0.812(1)	2.098(4)	2.908(5)	173.7(1)
O36-H362...O13 ^v	0.812(1)	2.586(4)	3.168(5)	129.7(1)
O37-H371...O29 ^v	0.811(1)	2.144(4)	2.896(5)	154.0(1)
O36-H361...O35 ^{vi}	0.822(1)	2.017(4)	2.821(5)	165.3(1)
O37-H371...O16 ^{vii}	0.811(1)	2.575(4)	3.136(5)	127.5(1)
O37-H372...O38 ^{viii}	0.815(1)	1.992(4)	2.798(5)	169.8(1)

Symmetry codes for **3**: (i) x, -1+y, z; (ii) 1-x, 1-y, -z; (iii) -1+x, -1+y, z. **5**: (i) x, -1+y, z; (ii) 1-x, 1-y, -z; (iii) -1+x, -1+y, z. **6**: (i) 2-x, -y, 1-z; (ii) x, -1+y, 1+z; (iii) 2-x, 1-y, -z; (iv) x, -1+y, z; (v) 1-x, 1-y, -z; (vi) x, y, -1+z; (vii) 1-x, -y, 1-z. **7**: (i) x, 1-y, 0.5+z; (ii) x, 1+y, z; (iii) 1-x, 1-y, 1-z; (iv) 0.5+x, 1.5-y, 0.5+z; (v) 1-x, y, 1.5-z. $\text{Ba}[(\text{NO}_2)_3\text{Ph-O}]_2 \cdot 6\text{H}_2\text{O}$: (i) -1+x, y, z; (ii) 1-x, -y, -z; (iii) 2-x, -y, 1-z; (iv) 1-x, -y, 1-z; (v) x, -1+y, z; (vi) 1+x, y, z; (vii) 2-x, -y, -z.

Table 6 Selected coordination geometry around the metal centre in Ba[(NO₂)₃Ph-O]₂*6H₂O (distances in Å and angles in °).

O1–Ba	2.724(3)	O33–Ba	2.735(3)
O9–Ba	2.935(3)	O34–Ba	2.821(3)
O17–Ba	2.728(3)	O35–Ba	2.789(3)
O28 ⁱ –Ba	3.002(3)	O36–Ba	2.823(3)
O32–Ba	3.070(3)	O37–Ba	2.799(3)
O1–Ba–O17	82.60(8)	O35–Ba–O9	155.04(8)
O1–Ba–O33	148.96(8)	O34–Ba–O9	129.92(8)
O17–Ba–O33	74.87(9)	O1–Ba–O28 ⁱⁱ	135.00(8)
O1–Ba–O35	127.63(8)	O17–Ba–O28 ⁱⁱ	141.85(8)
O17–Ba–O35	86.11(8)	O33–Ba–O28 ⁱⁱ	71.91(9)
O33–Ba–O35	72.37(8)	O35–Ba–O28 ⁱⁱ	66.44(8)
O1–Ba–O37	77.01(8)	O37–Ba–O28 ⁱⁱ	69.96(8)
O17–Ba–O37	125.60(8)	O1–Ba–O32	63.41(8)
O33–Ba–O37	133.70(8)	O17–Ba–O32	54.62(8)
O35–Ba–O37	68.96(8)	O33–Ba–O32	116.29(9)
O1–Ba–O34	108.88(8)	O35–Ba–O32	68.45(8)
O17–Ba–O34	111.44(8)	O37–Ba–O32	71.17(8)
O33–Ba–O34	61.99(9)	O34–Ba–O33	61.13(8)
O35–Ba–O34	122.80(8)	O34–Ba–O9	64.68(8)
O37–Ba–O34	122.81(9)	O36–Ba–O9	69.81(8)
O1–Ba–O36	63.70(8)	O34–Ba–O28 ⁱⁱ	67.92(8)
O17–Ba–O36	137.08(8)	O36–Ba–O28 ⁱⁱ	78.06(8)
O33–Ba–O36	122.12(9)	O9–Ba–O28 ⁱⁱ	131.22(8)
O35–Ba–O36	135.15(8)	O34–Ba–O32	163.52(8)
O37–Ba–O36	73.81(8)	O36–Ba–O32	121.23(8)
O1–Ba–O9	56.52(8)	O9–Ba–O32	100.02(7)
O17–Ba–O9	69.57(8)	O28 ⁱⁱ –Ba–O32	128.20(7)
O33–Ba–O9	95.12(8)		

Symmetry codes: (i) x, 1+y, z; (ii) x, -1+y, z.

Table 7 Thermodynamic and explosive properties of formulations of energetic salts of the [(CH₃)₂N(CH₂Cl)NH₂]⁺ cation with ammonium nitrate (AN). All formulations contain 1% of TFNA = trifluoro-trinitro-azahexane.

	AN + 2 ^a	AN + 3 ^a	AN + 4 ^a	AN + 5 ^a	AN + 7 ^a	AN + 8 ^a	AN + 9 ^a
ρ (g cm ⁻³) ^b	1.670	1.714	1.676	1.668	1.692	1.706	1.692
M (g mol ⁻¹)	101.23	119.41	92.74	94.43	127.49	133.53	99.05
Ω (%) ^c	+0.38	+0.15	-0.35	-0.50	+0.61	-0.37	-0.46
ΔU_f° / kJ kg ^{-1d}	-3258	-2296	-3185	-3345	-2956	-3392	-3394
ΔH_f° / kJ kg ^{-1e}	-3393	-2425	-3322	-3480	-3091	-3521	-3531
T_{ex} / K ^f	3142	3609	2980	3048	3124	3143	2926
V_0 / L kg ^{-1g}	942	910	957	944	948	910	955
P_{det} / kbar ^h	259	279	264	234	266	256	266
D / m s ⁻¹ⁱ	8085	8347	8137	7942	8194	8019	8182
I_{sp} (s) ^j	230	245	229	221	238	227	229

^a 78% AN + 21% **2**; 70% AN + 29% **3**; 84% AN + 15% **4**; 86% AN + 13% **5**; 84% AN + 15% **7**; 79% AN + 20% **8**; 84% AN + 15% **9**; ^b Density (averaged with EXPLO5); ^c Oxygen balance according to EXPLO5; ^d Calculated energy of formation; ^e Calculated enthalpy of formation; ^f Temperature of the explosion gases; ^g Volume of the explosion gases; ^h Detonation pressure; ⁱ Detonation velocity; ^j Specific impulse (isobaric combustion for the mixture at a chamber pressure = 60.0 bar).

Table 8 Thermodynamic and explosive properties of formulations of energetic salts of the $[(\text{CH}_3)_2\text{N}(\text{CH}_2\text{Cl})\text{NH}_2]^+$ cation with ammonium dinitramide (ADN). All formulations contain 1% of TFNA = trifluoro-trinitro-azaahexane.

	ADN + 2 ^a	ADN + 3 ^a	ADN + 4 ^a	ADN + 5 ^a	ADN + 7 ^a	ADN + 8 ^a	ADN + 9 ^a
ρ (g cm ⁻³) ^b	1.720	1.767	1.737	1.727	1.752	1.767	1.7055
M (g mol ⁻¹)	137.94	155.32	130.54	133.83	174.83	176.85	138.11
Ω (%) ^c	+0.12	-0.09	+0.45	-0.24	+0.28	+0.06	+0.29
ΔU_f° / kJ kg ⁻¹ ^d	-549	+275	-178	-331	+100	-687	-489
ΔH_f° / kJ kg ⁻¹ ^e	-669	+160	-299	-449	-19	-800	-610
T_{ex} / K ^f	4055	4533	3900	4033	4133	4054	3881
V_0 / L kg ⁻¹ ^g	877	845	890	872	878	837	888
P_{det} / kbar ^h	329	338	330	305	334	332	337
D / m s ⁻¹ ⁱ	8649	8809	8780	8584	8733	8634	8840
I_{sp} (s) ^j	253	259	250	231	255	248	249

^a 73% ADN + 26% **2**; 64% ADN + 35% **3**; 81% ADN + 18% **4**; 83% ADN + 16% **5**; 80% ADN + 19% **7**; 75% AN + 24% **8**; 81% ADN + 18% **9**; ^b Density (averaged with EXPLO5); ^c Oxygen balance according to EXPLO5; ^d Calculated energy of formation; ^e Calculated enthalpy of formation; ^f Temperature of the explosion gases; ^g Volume of the explosion gases; ^h Detonation pressure; ⁱ Detonation velocity; ^j Specific impulse (isobaric combustion for the mixture at a chamber pressure = 60.0 bar).

References

- 1 J. Thiele, *Just. Lieb. Ann. Chem.*, 1892, **270**, 54–63; J. Thiele and J. T. Marais, *Just. Lieb. Ann. Chem.*, 1893, **273**, 144–160; J. Thiele, *Ber. Dtsch. Chem. Ges.*, 1893, **26**, 2645–2646; J. Thiele, *Just. Lieb. Ann. Chem.*, 1898, **303**, 57–75.
- 2 A. Hammerl, G. Holl, T. M. Klapötke, P. Mayer, H. Nöth, H. Piotrowski and M. Warchhold, *Eur. J. Inorg. Chem.*, 2002, 834–845.
- 3 C. Miró Sabaté, E. Jeanneau and J. Stierstorfer, *Z. Anorg. Allg. Chem.* 2011, **637(11)**, 1490–1501.
- 4 Y. Inoue, M. Ouchi and T. Hakushi, *Bull. Chem. Soc. Japan*, 1985, **58**, 525–530.
- 5 CrysAlis Pro, Oxford Diffraction Ltd., Version 4, 2004.
- 6 SIR-92, A program for crystal structure solution A. Altomare, G. Cascarano, C. Giacovazzo and A. Guagliardi, *J. Appl. Crystallogr.*, 1993, **26**, 343.
- 7 G. M. Sheldrick, SHELXS-97, Program for Crystal Structure Solution, Universität Göttingen, 1997.
- 8 G. M. Sheldrick, SHELXL-97, Program for the Refinement of Crystal Structures, University of Göttingen, Germany, 1997.
- 9 L. J. Farrugia, *J. Appl. Crystallogr.*, 1999, **32**, 837.
- 10 A. L. Spek, PLATON, A Multipurpose Crystallographic Tool, Utrecht University, Utrecht, The Netherlands, 1999.
- 11 SCALE3 ABSPACK-An Oxford Diffraction program (1.0.4,gui:1.0.3), © 2005 Oxford Diffraction Ltd.
- 12 A. Xia and P. R. Sharp, *Inorg. Chem.*, 2001, **40(16)**, 4016–4021.

- 13 A copy of the cif files of compounds **3**, **6**, **7**, **8** and Ba[(NO₂)₃Ph-O]₂*6H₂O can be obtained free of charge on application to The Director, CCDC, 12 Union Road, Cambridge CB2 1EZ, UK (Fax: int. code_(1223)336-033. E-mail for inquiry: fileserv@ccdc.cam.ac.uk. E-mail for deposition: deposit@ccdc.cam.ac.uk).
- 14 W. H. Beamer, *J. Am. Chem. Soc.*, 1948, **70**, 2979.
- 15 International Tables for X-Ray Crystallography, vol. III, Kynoch Press, Birmingham, 1962, p. 270.
- 16 T. M. Klapötke, P. Mayer and J. Stierstorfer, *Phosphorus, Sulfur Silicon Relat. Elem.*, 2009, **184(9)**, 2393–2407
- 17 K. Karaghiosoff, T. M. Klapötke and C. Miró Sabaté, *Eur. J. Inorg. Chem.*, 2009, 238–250.
- 18 A. Hammerl, G. Holl, T. M. Klapötke, P. Mayer, H. Nöth, H. Piotrowski and M. Warchhold, *Eur. J. Inorg. Chem.*, 2002, 834–845.
- 19 T. M. Klapötke and C. Miró Sabaté, *Eur. J. Inorg. Chem.*, 2008, **34**, 5350–5366; T. M. Klapötke, C. Miró Sabaté, *Z. Anorg. Allg. Chem.*, 2008, **634**, 1017–1024.
- 20 Gaussian 03W Program, Gaussian Inc., Wallingford, CT, 2004.
- 21 A.P. Scott and L. Radom, *J. Phys. Chem.*, 1996, **100**, 16502.